Journal of Multidisciplinary Engineering Science Studies (JMESS)
ISSN: 2458-925X
Vol. 3 Issue 4, April - 2017

Calculate The Density And The Potential Energy When Charge Particle Channeling In Single And Double Carbon Nanotubes

Bahaa H. Abbass , Khalid A. Ahmad , Riyahd K. Ahmed
Al-Mustansiriyah University, College of Science, Department of Physics.
Baghdad-Iraq
ahmed_naji_abd@yahoo.com

***Abstract*—To investigate the wake effects in the transport of charged particles through single-walled (SWCNT) and double-walled (DWCNTs) carbon nanotubes, by using a semiclassical kinetic model, with the introduction of electron band structure effect. The analytical expressions of the induced electron density at nanotube surface and the induced potential around the nanotube walls are obtained. The results indicate that a bell-like distribution appears for the induced electron density when the incident particle speed is below a threshold value, otherwise wake-like oscillation can be seen behind the particle in the axial distribution. Dependencies of the amplitude and frequency of oscillations on the incident particle speed are. Meanwhile, it is noted that the valence electrons in the outer wall of DWCNTs tend to be easily excited by the polarized electrons on the inner wall, compared with that by the incident particle without the inner wall in SWCNTs. Finally, the induced potential trailing the incident particle also exhibits remarkable oscillations, not only along the axial direction but also in the lateral region, with evident extrema at the nanotube walls.**

Keywords—carbon nanotube, potential energy, self-energy

Introduction

Carbon nanotubes (CNTs) are systems of unquestionable technological interest. Because their low dimensionality, nanometer size and remarkable electronic, mechanic and magnetic properties, nanotubes are promising structures for several purposes in many fields of physics, materials science, or biomedicine [1].

It's known, carbon nanotubes can exhibit either metallic or semiconducting properties, associated with the rolling pattern of a planar sheet to a cylindrical cavity. Consequently, dependent on the actual geometrical structure, the energy band structure of the electrons on the nanotube wall should be introduced in the theoretical investigation on the interaction of ions with nanotubes. [2]

A semiclassical kinetic model was proposed to describe the electromagnetic processes in carbon nanotubes for various band structures,[2] where the electron dispersion relation is in the framework of the tight-binding model.[3] Through the adoption of this kinetic model combined with the dielectric response theory, the collective excitation of the surface electrons studied through the transport of a charged particle in the zigzag and armchair nanotubes of metallic character in previous works.[4,5] Then, the theoretical model was extended to describe the electronic excitation in 2WCNTs.[6] The analytical expressions of the self energy and stopping power were also obtained, which can manifest the local features of the induced potential where the ions are located.

In this study, the kinetic model will be extended to focus special interesting the wake effects of the induced electron density and induced potential, with charged particles moving in both SWCNTs and DWCNTs of metallic character. The valence electrons are perturbed by charged particle passing, bringing about electron polarization.

When carbon nanotubes are in equilibrium state, the valence electrons on the walls meet the Fermi equilibrium distribution.[2] As well, □ electrons are the only electrons cared about for their significant effects on electronic properties. Atomic units (a.u.) will be used throughout this paper. Both SWCNT and DWCNT are considered as infinitely long and infinitesimally thin cylindrical shells. The SWCNT with radius □, and the DWCNT consists of tow coaxial walls with the inner radius $\mathbf{a_1}$ and the outer radius $\mathbf{a_2}$, respectively. The cylindrical coordinate system □ = (□, φ, □) used here, with the orientation of □ parallel to the axis of nanotubes. Considering a charged particle □ tracking parallel to the axis of SWCNT or DWCNT at constant speed □, It is confirmed that the particle instantaneous position is given by $\boldsymbol{r_0} = (\rho_0, \boldsymbol{\varphi_0}, \mathbf{t})$, here $\rho_0 < a$ and $\rho_0 < \mathbf{a_1}$.

The samples $\boldsymbol{\varphi_1^1}$, $\boldsymbol{\varphi_2^1}$ express to the total potential inside (□ < □) and outside (□ > □) the nanotube, while the value of the inside potential can be expressed as $\boldsymbol{\varphi_1^1} = \boldsymbol{\varphi_0^1} + \boldsymbol{\varphi_{ind}^1}$.

The induced potential $\boldsymbol{\varphi_{ind}^1}$ is caused by the charge polarization on the nanotube surface and the potential $\boldsymbol{\varphi_0^1}$ represents the Coulomb potential from the moving charged particle itself, which can be expanded in terms of cylindrical Bessel functions $\boldsymbol{I_m(x)}$ and $\boldsymbol{K_m(x)}$. According to the work of Ref. [7], the induced potential $\boldsymbol{\varphi_{ind}^1}$and $\boldsymbol{\varphi_2^1}$ can be given as follows

$$\boldsymbol{\varphi_{ind}^1}(\boldsymbol{\rho}, \emptyset, \boldsymbol{z}, \boldsymbol{t}) = \frac{Q}{\pi}\sum_{m=-\infty}^{\infty} \boldsymbol{dke^{ik(z-vt)+im(\emptyset-\emptyset_0)}} * I_m(k\,\boldsymbol{\rho_0})I_m(k\boldsymbol{\rho})\boldsymbol{A_m(k)}, \text{ for } □ < □ \quad \textbf{(1)}$$

$\varphi_2^1(\rho, \emptyset, z, t) = \frac{Q}{\pi}\sum_{m=-\infty}^{\infty} dke^{ik(z-vt)+im(\emptyset-\emptyset_0)} * I_m(k\rho_0)K_m(k\rho)B_m(k)$, for □ > □ **(2)**

Where, **[8]**

$A_m(k) = \frac{K_m(ka)}{I_m(ka)}[\epsilon^{-1}(k, m, \omega, a) - 1]$, **(3)**

$B_m(k) = \epsilon^{-1}(k, m, \omega, a)$, **(4)**

With k the longitudinal wave number, m the angular momentum. [9]

The dielectric function $\epsilon(k, m, \omega, a)$ of electron can be expressed in term of response function $\chi(k, m, \omega, a)$ which has different expressions for zigzag and armchair nanotubes.

Thus, can be calculated the induced potential and other relevant quantities by using the above expressions for the coefficients A_m and B_m [10]

$\epsilon(k, m, \omega, a) = 1 - 4\pi a I_m(ka)K_m(ka)\chi(k, m, \omega, a)$, **(5)**

With $4\pi a I_m(ka)\ K_m(ka)$ is the Fourier transform of the electron-electron Coulomb interaction on the surface of nanotube. **(□, □, □, □)** of the last term is the response function of the carbon nanotubes with various expressions for zigzag and armchair nanotubes owing to the distinctive energy band structure, with □ being the frequency of the elementary excitation. So, the dielectric function obtained here is not only related to the longitudinal wave number k, the angular momentum m, the frequency ω of the elementary excitation, and the radius of the nanotube a, but also the chiral angle of the nanotube which indicates the different energy dispersion relation of electrons.[4]

So, $\chi(k, m, \omega, a)$ for zigzag:

$\chi(k, m, \omega, a) = \frac{4}{\pi\hbar}\frac{1}{\sqrt{3}nb}\sum_{s=1}^{n}\int_{-2\pi/3b}^{2\pi/3b} dp_z \frac{\partial f_0}{\partial\varepsilon}\frac{\left(\frac{m}{a}\right)v_\phi + kv_z}{\left(\frac{m}{a}\right)v_\phi + kv_z - \omega - i\gamma}$, **(6)**

and for armchair**:**

$\chi(k, m, \omega, a) = \frac{4}{\pi\hbar}\frac{1}{3nb}\sum_{s=1}^{n}\int_{-2\pi/\sqrt{3}b}^{2\pi/\sqrt{3}b} dp_z \frac{\partial f_0}{\partial\varepsilon}\frac{\left(\frac{m}{a}\right)v_\phi + kv_z}{\left(\frac{m}{a}\right)v_\phi + kv_z - \omega - i\gamma}$, **(7)**

With $f_0(p) = \frac{1}{1+\exp\left\{\frac{\varepsilon(p)}{k_B T}\right\}}$ The electrons of the nanotube surface are supposed to meet the Fermi equilibrium distribution function, with the chemical potential of graphite being null valued, where $\varepsilon = \varepsilon(p)$ is the electron energy with respect to Fermi level, **p** is the electron's two- dimensional quasimomentum tangential to the nanotube's surface. k_B is the Boltzmann constant, T is the temperature which remains at **273 K** here. [10] And $v_z = \frac{\partial\varepsilon}{\partial p_z}$, but v_ϕ, Taking into consideration the p_ϕ a quantized variable, and approximate the partial derivative with finite difference, $v_\phi = \varepsilon[p_z, p_\phi(s+1)] - \varepsilon[p_z, p_\phi(s)]$, where p_z and p_ϕ are the projections of **p** on the axis and the *z* direction of the nanotube and (s)=1,2,.n for zigzag(n,0) or armchair (n, n). [10,11]

Substituting Eq.s (3,4) in (1,2), the induced potential inside the nanotube can be written as:[11]

$\varphi_{ind}^1 = \frac{Q}{\pi}\sum_{m=-\infty}^{\infty}\int_{-\infty}^{+\infty} dke^{ik(z-vt)+im(\emptyset-\emptyset_0)} I_m(k\rho_0)I_m(k\rho)\frac{K_m(ka)}{I_m(ka)}[\epsilon^{-1}(k, m, \omega, a) - 1]$, **(8)**

And

$\varphi_2^1 = \frac{Q}{\pi}\sum_{m=-\infty}^{\infty}\int_{-\infty}^{+\infty} dke^{ik(z-vt)+im(\emptyset-\emptyset_0)} I_m(k\rho_0)K_m(k\rho)[\epsilon^{-1}(k, m, \omega, a)]$, (**9**)

The induced electron density □1 on the surface of the nanotubes is obtained as follows:

$n^1 = \frac{Q}{\pi}\sum_{m=-\infty}^{\infty}\int_{-\infty}^{+\infty} dke^{ik(z-vt)+im(\emptyset-\emptyset_0)} I_m(k\rho_0)K_m(ka)[\epsilon^{-1}(k, m, \omega, a)]\chi(k, m, \omega, a)$, **(10)**

Likewise, for DWCNTs, use φ_1^2 , φ_2^2 and φ_3^2 to express the total potential inside the inner wall (□ < a_1), the potential between two walls (a_1 < □ < a_2), and the potential outside the outer wall (a_2 < □), respectively.

The potential $\varphi_1^2 = \varphi_0^2 + \varphi_{ind}^2$ is similar to φ_1^1 , the Coulomb potential from the moving charged particle itself, which could be expanded in terms of cylindrical Bessel functions $I_m(x)$ and $K_m(x)$. On the basis of previous work, these potentials can be given by :[6]

$\varphi_{ind}^2 = \frac{Q}{\pi}\sum_{m=-\infty}^{\infty}\int_{-\infty}^{+\infty} dke^{ik(z-vt)+im(\emptyset-\emptyset_0)} I_m(k\rho_0)I_m(k\rho)\frac{K_m(ka_1)}{I_m(ka_1)}\{[\epsilon^{-1}(k, m, \omega, a_j)][1 -$

$4\pi a_2 I_m(ka_2)K_m(ka_2)\chi(k, m, \omega, a_2) + \frac{4\pi a_2 K_m^2(ka_2)I_m(ka_1)}{K_m(ka_2)}\chi(k, m, \omega, a)$**-1},** for ρ < a_1 **(11)**

$\varphi_2^2 = \frac{Q}{\pi}\sum_{m=-\infty}^{\infty}\int_{-\infty}^{+\infty} dke^{ik(z-vt)+im(\emptyset-\emptyset_0)} I_m(k\rho_0)[\epsilon^{-1}(k, m, \omega, a_j)][[1_- 4\pi a_2 I_m(ka_2)K_m(ka_2)\chi(k, m, \omega, a_2) +$

$4\pi a_2 K_m^2(ka_2)\chi(k, m, \omega, a_2)I_m(k\rho)]$, for a_1 < □ < a_2 **(12)**

$\varphi_3^2 = \frac{Q}{\pi}\sum_{m=-\infty}^{\infty}\int_{-\infty}^{+\infty} dke^{ik(z-vt)+im(\emptyset-\emptyset_0)} I_m(k\rho_0)K_m(ka)[\epsilon^{-1}(k, m, \omega, a_j)]$, for a_2 < □ **(13)**

Where j **= 1, 2** and

$$\epsilon(k,m,\omega,a) = [1 - 4\pi a_1 I_m(ka_1)K_m(ka_1).\chi(k,m,\omega,a_1)][1 - 4\pi a_2 I_m(ka_2)K_m(ka_2).\chi(k,m,\omega,a_2)] - [4\pi a_1 I_m(ka_1)K_m(ka_2)]^2 a_1 a_2.\chi(k,m,\omega,a_1)\chi(k,m,\omega,a_2), (14)$$

Then the induced electron density n_j^2 is obtained as follows:

$$n_j^2 = \frac{Q}{\pi}\sum_{m=-\infty}^{\infty}\int_{-\infty}^{+\infty} dke^{ik(z-vt)+im(\emptyset-\emptyset_0)} I_m(k\,\rho_0)[\epsilon^{-1}(k,m,\omega,a_j)\chi(k,m,\omega,a_j)\{[1 - 4\pi a_2 I_m(ka_2)K_m(ka_2)\chi(k,m,\omega,a_2)]K_m(ka_j) + 4\pi a_2 K_m^2(ka_2)\chi(k,m,\omega,a_2)I_m(ka_j),$$ □ = (1,2) **(17)**

Present work, the accounts are considered the charged particle as a proton (□ **= 1**) tracking along the axis ($\rho_0 = 0$) of SWCNT or DWCNT. The friction coefficient is set at □ **= 0.001**□□, with the classical plasma frequency in homogeneous electron gas $\omega_p = (4\pi n_0/a)^{1/2}$**.** Here n_0 is the surface density of the valence electrons. As well as, for the case of axial symmetry, only □ **= 0** can be used on in the investigation.

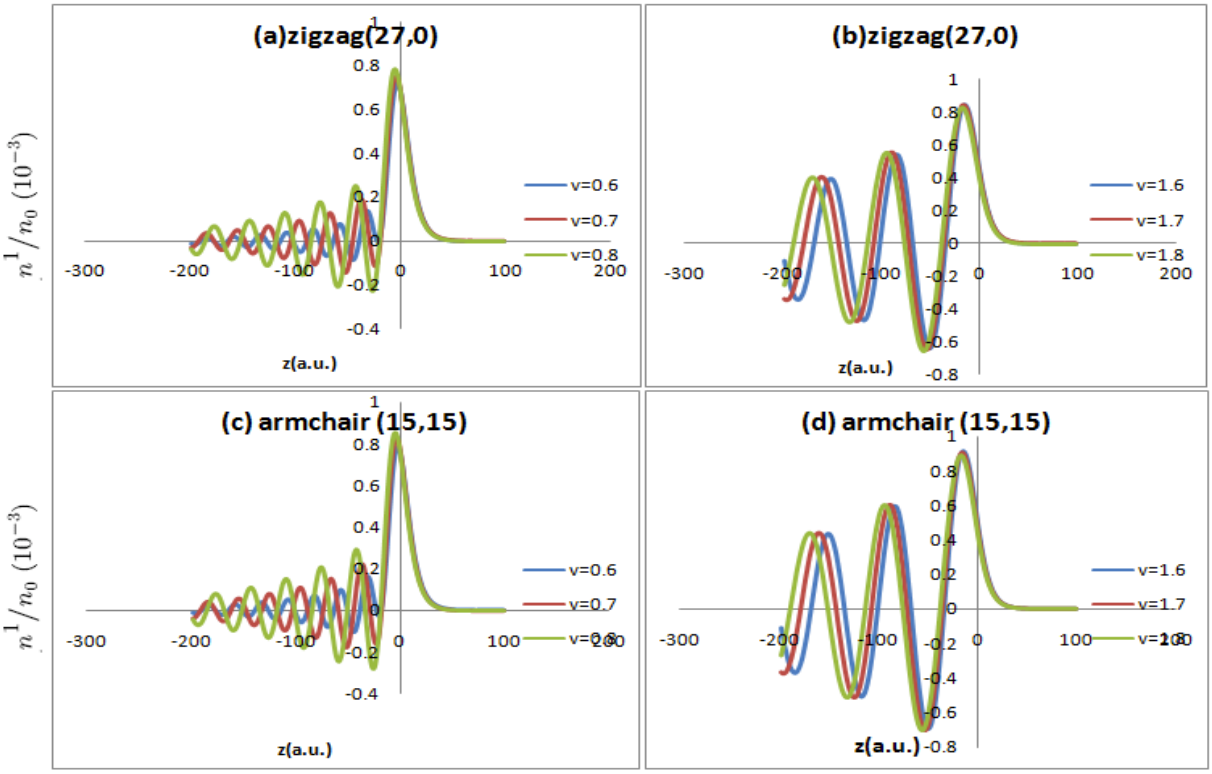

Fig. 1. The rate of the induced electron density (n^1/n_0) dependent on the axial position □ in the plane φ = φ $_0$ as the proton moves along the axis of zigzag (27,0) and armchair (15,15) SWCNT respectively, at lower speeds □ = 0.6, 0.7, 0.8 a.u. in (a) and (c), or higher speeds □ = 1.6, 1.7, 1.8 a.u. in (b) and (d).

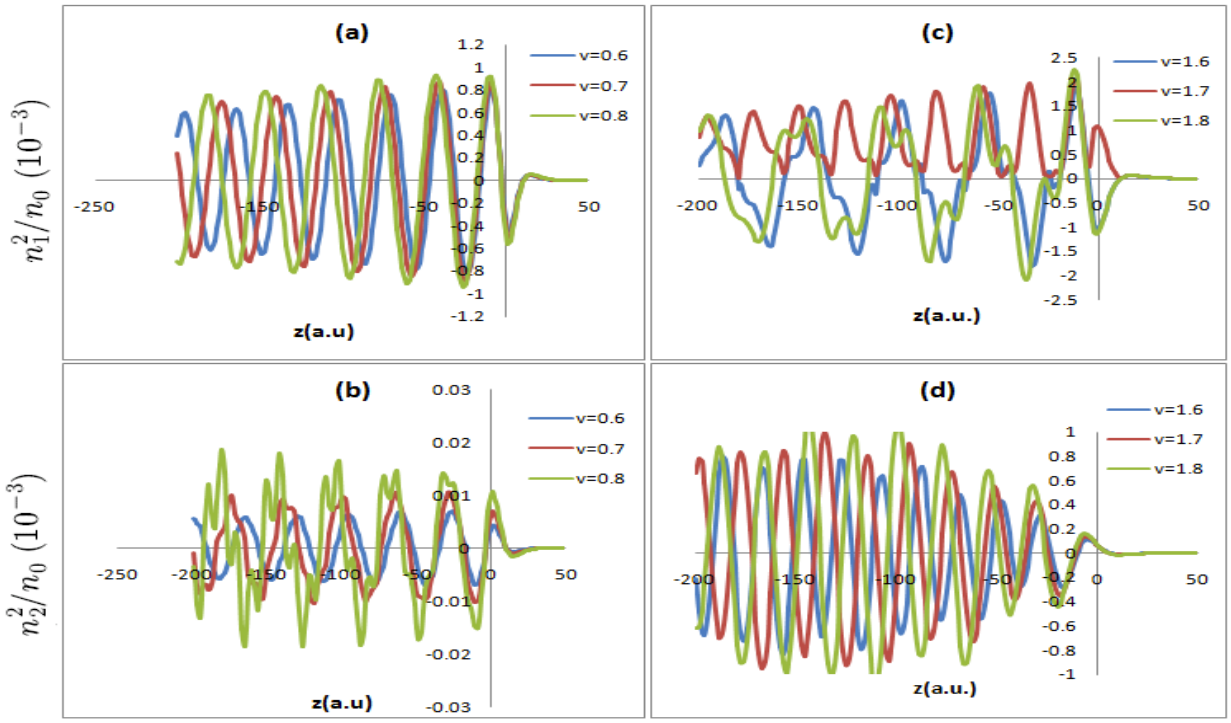

Fig.2. The rate of the inner $\frac{n_0^2}{n_0}$ and outer $\frac{n_2^2}{n_0}$ induced electron densities dependent on the axial position □ in the plane □ = φ_0, as the proton moves along the axis of zigzag (15,0)–zigzag (27,0) DWCNT, at lower speeds □ = 0.6, 0.7, 0.8 a.u. in (a) and (b), and higher speeds □ = 1.6, 1.7, 1.8 a.u. in (c) and (d).

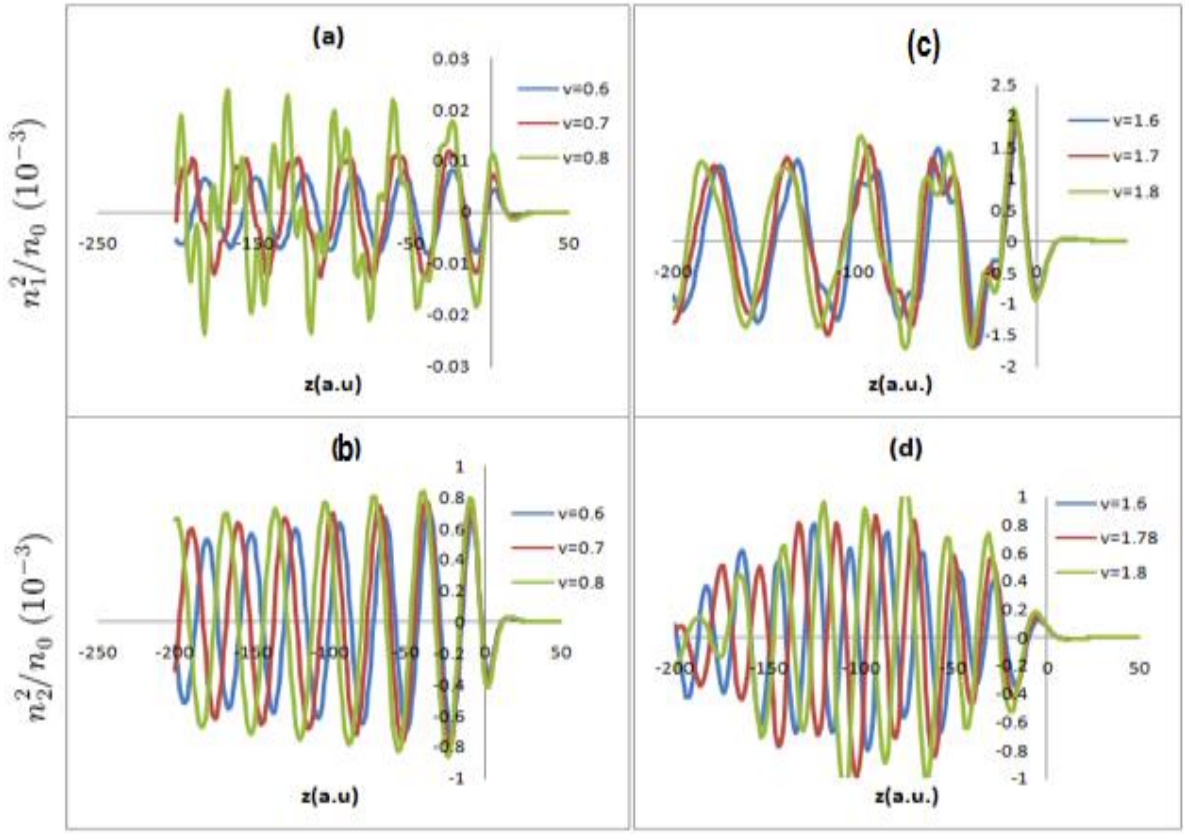

Fig. 3. Similar simulation results as those in Fig. 2, but in armchair (9,9)–armchair (15,15) 2WCNT.

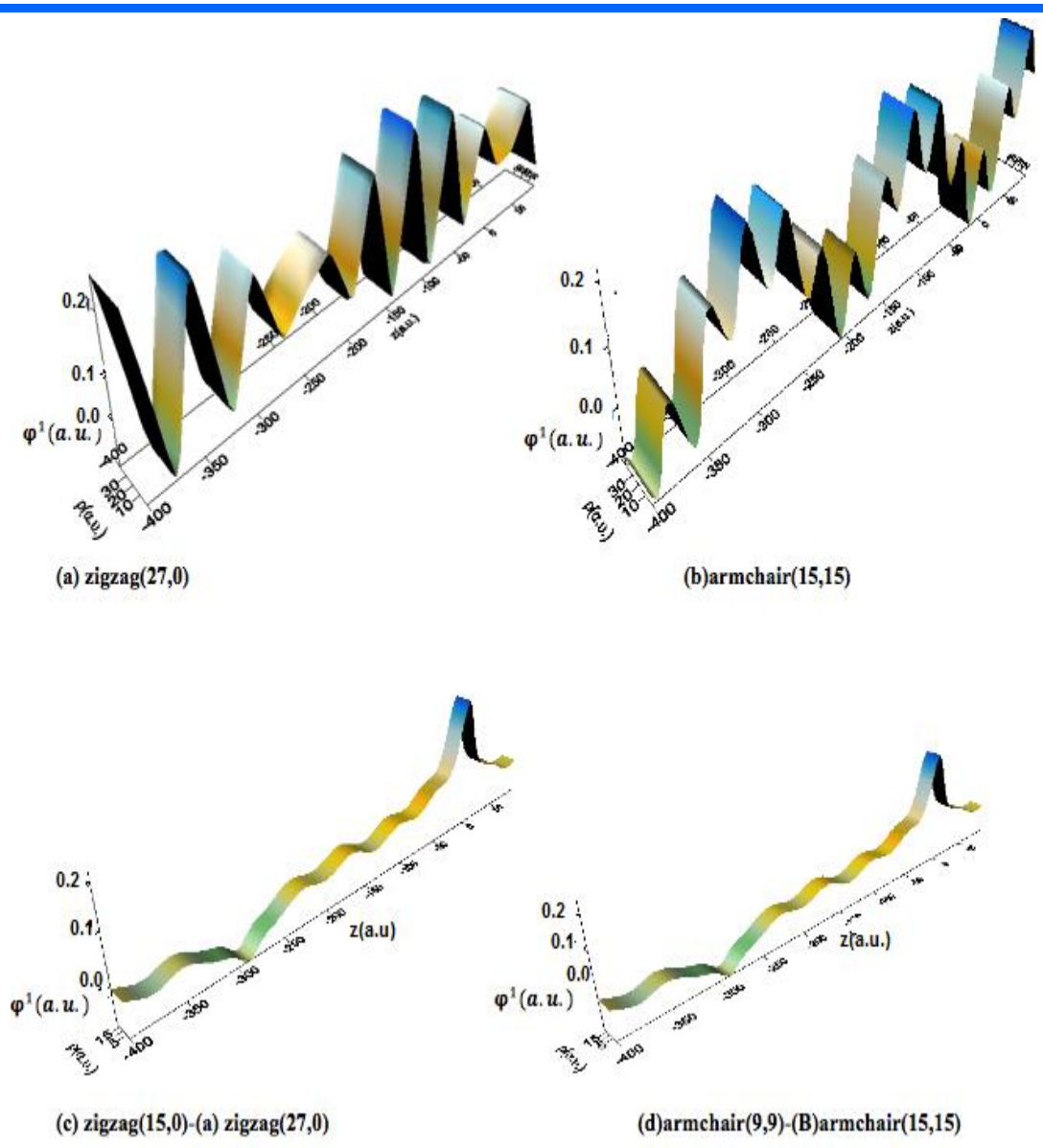

Fig.4. Total potentials φ^1 of SWCNT versus □ and □ positions for (a) zigzag (27,0) nanotube and (b) armchair (15,15) nanotube, and φ^2 of DWCNT for (c) zigzag (15,0)- zigzag (27,0) and (d) armchair (9,9)-armchair (15,15) nanotubes, induced by the proton moving along the axis of the nanotubes at fixed initial speed □ = 1.7 a.u.

Conclusion

Figure 1 exhibits the SWCNT induced electron density ratio $\frac{n^1}{n^0}$ opposite the axial position □ in the plane $\boldsymbol{\varphi = \varphi_0}$, for zigzag (27,0) nanotube with radius □ **= 20.25** a.u. and armchair (15,15) nanotube with □ **= 20.79** a.u. can be observed that there exists a threshold value for the proton speed about □ **= 0.7** a.u. from Figs. 1(a) and 1(c). When the projectile proton's speed is under the threshold value, the induced electron density exhibits a bell-like distribution, while over the threshold value; wake-like oscillations can be observed in the axial distribution for both metallic nanotubes, as exhibited in Figs. 1(b) and 1(d). In accordance to Ref. [12], the collective excitation, i.e. the usual wake oscillations, might happen only when the particle speed matches the phase velocity of the plasmons of CNTs, Due to the Landau damping.

Moreover, making a comparison from Figs. 1(a) and 1(b), 1(c) and 1(d), obtained that as the particle speed increases, the amplitude of oscillations increases in magnitude when trailing at slower speeds, but decreases in the higher speed range. At the same time, the frequency of oscillations keeps decreasing with the increasing particle speeds. Moreover, it can also be noticed that the positions of the first peak of trailing oscillations shift to the opposite direction of the □ axis as the speed increases, for all the induced electron density curves at lower speeds and higher speeds.

For DWCNTs, the rate of inner induced electron density $\frac{n_1^2}{n_0}$ and outer induced electron density $\frac{n_2^2}{n_0}$ versus axial direction in the plane $\boldsymbol{\varphi} = \boldsymbol{\varphi_0}$in Figs. 2 and 3. Here, two DWCNTs are chosen: with inner zigzag (15,0) ($\boldsymbol{a_1}$ **= 11.25** a.u.) and outer zigzag (27,0) ($\boldsymbol{a_2}$ **= 20.25** a.u.) in Fig. 2, or inner armchair (9,9) ($\boldsymbol{a_1}$ **= 11.69** a.u.) and outer armchair (15,15) ($\boldsymbol{a_2}$ **= 20.79** a.u.) in Fig. 3.

Induced electron densities $\frac{n_1^2}{n_0}$ and $\frac{n_2^2}{n_0}$ depended on the axial position and the projectile speed are like to those in SWCNTs. From Figs. 2(b) and 2(d), the valence electrons on the outer walls are largely excited by the inner polarized electrons which are induced by the incident charge particle.

These excitations are stronger than those which are perturbed directly by the intruding particle without the inner walls, as shown in Figs. 1(a) and 1(b) in the zigzag (27,0) nanotube, leading to larger amplitude of the wake oscillation and smaller wavelength. Results similar can also can be found at outer wall of armchair (9,9)-armchair (15,15) nanotube shown in Figs. 3(b) and 3(d), compared with the results in armchair (15,15) nanotube in Figs. 1(c) and 1(d). So, it can be inferred that the incident ion would expose larger energy loss from the excitation of the outer nanotube than that without an inner wall. Reality, in the previous work,[5] founded that the energy the incident ion loses in a DWCNT is much larger than that in the outer SWCNT, but smaller than that in the inner SWCNT, owing to the strong interference effects between the two walls in the DWCNT.

The Three-dimensional 3D it shows the spatial variation of the total potential, while the proton moves along the tube axis in Fig.4. Figures 4(a) and 4(b) display the total potential $\boldsymbol{\varphi_1^1}$ and $\boldsymbol{\varphi_2^1}$ inside and outside of zigzag (27,0) and armchair (15,15) nanotubes, respectively, at the fixed impact speed **o = 1.7** a.u. From the figures, there is a quite pronounced oscillation behind the particle along the direction. Owing to the existence of the electron polarization induced by the proton, the oscillating wake potential exhibits a local extremum on the surface of nanotube wall (=), which becomes decaying significantly inside (<) and outside (>) nanotubes. The total potentials $\boldsymbol{\varphi^2}$ of DWCNT for the proton moving along the axis of zigzag (15,0)-zigzag (27,0) nanotubes and armchair (9,9)-armchair (15,15) nanotubes at the same incident speed are also investigated, as shown in Figs. 4(c) and 4(d). Same to the case in SWCNTs, local extrema around the inner and outer walls of nanotubes along the direction are displayed, and the excitations of valence electrons on the outer walls induced by polarized electrons on the inner walls can be noticed clearly.

Briefly, based on a semi-classical kinetic theory combined with the dielectric response theory, investigated wake effects in proton transport through SWCNTs and DWCNTs. The analytical expressions of the induced electron density and spatial potential have been derived, while considering the real band-structure of electrons on the nanotubes surface. The simulation results that the induced electron density strongly depends on the projectile speed. A wake-like oscillation can be found in the axial distribution as the projectile speed is set above a threshold speed value. As well as, corresponding to the features of the induced electron density on the surface of nanotubes, the induced potential behind the incident particle also presents oscillations not only along the axial direction but also in the lateral region. There appear local extrema located at the walls of SWCNT and DWCNT. The kinetic model will be adopted in future studies of charged particle channeling in or between walls of the multiwall nanotubes, especially with different nanotube chiral angle.

References

1. Slepyan G Ya, Maksimenko S A, Lakhtakia A, Yevtushenko O and Gusakov A V 1999 Phys. Rev. B 60 17136.
2. Zhu Z Y, Zhu D Z, Lu R R, Xu Z J, Zhang W and Xia H 2005 Proc. SPIE 5974 597413.
3.Saito R, Fujita M, Dresselhaus G and Dresselhaus M S 1992 Phys. Rev. B 46 1804.
4. Zhao D, Song Y H and Wang Y N 2008 Chin. Phys. Lett.25 2588
5. Song Y H, Zhao D and Wang Y N 2008 Phys. Rev. A 78012901.
6. You S Y, Song Y H and Wang Y N 2009 Nucl. Instrum. Methods Phys. Res. Sect. B 267 3133.
7. Wang Y N and Mišković Z L 2004 Phys. Rev. A 69 022901.
8. Y. N. Wang and Z. L. Mišković, 2004 Phys. Rev. A 69, 022901.
9. T. Sto¨ckli, J.M. Bonard, A. Chaˆtelain, Z.L. Wang, and P. Stadelmann 2001,Phys. Rev. B 64, 115424.
10. Y.N. Wang and Z.L. Misˇkovic´2002 Phys. Rev. A 66, 042904.
11. Y.H. Song, Z.D., and Y.N. Wang 2008 Phy. Rev. A 78, 012901.
12. Radović I, Borka D and Mišković Z L 2011 Phys. Lett. A 375 3720.